of malignant pheochromocytoma and malignant paraganglioma. The escalation of ^{123}I-MIBG doses might be beneficial for the diagnosis of distribution of metastasis.

Acknowledgements

This research did not receive any support in the form of grants, equipment, drugs, or combination of these.
This research did not receive any funding from any of the following organizations: National Institutes of Health, Wellcome Trust, Howard Hughes Medical Institute, and others.

Conflicts of interest

There are no conflicts of interest.

References

1 Jaques S Jr., Tobes MC, Sisson JC. Sodium dependency of uptake of norepinephrine and m-iodobenzylguanidine into cultured human pheochromocytoma cells: evidence for uptake-one. *Cancer Res* 1987; **47**:3920–3928.
2 Ilias I, Pacak K. Current approaches and recommended algorithm for the diagnostic localization of pheochromocytoma. *J Clin Endocrinol Metab* 2004; **89**:479–491.
3 Wieland DM, Wu J, Brown LE, Mangner TJ, Swanson DP, Beierwaltes WH. Radiolabeled adrenergic neuron-blocking agents: adrenomedullary imaging with [131I]iodobenzylguanidine. *J Nucl Med* 1980; **21**:349–353.
4 Nakajo M, Shapiro B, Copp J, Kalff V, Gross MD, Sisson JC, *et al.* The normal and abnormal distribution of the adrenomedullary imaging agent m-[I-131]iodobenzylguanidine (I-131 MIBG) in man: evaluation by scintigraphy. *J Nucl Med* 1983; **24**:672–682.
5 Sisson JC, Frager MS, Valk TW, Gross MD, Swanson DP, Wieland DM, *et al.* Scintigraphic localization of pheochromocytoma. *N Engl J Med* 1981; **305**:12–17.
6 Shapiro B, Copp JE, Sisson JC, Eyre PL, Wallis J, Beierwaltes WH. Iodine-131 metaiodobenzylguanidine for the locating of suspected pheochromocytoma: experience in 400 cases. *J Nucl Med* 1985; **26**:576–585.
7 Sisson JC, Shulkin BL. Nuclear medicine imaging of pheochromocytoma and neuroblastoma. *Q J Nucl Med* 1999; **43**:217–223.
8 Rufini V, Castaldi P, Treglia G, Perotti G, Gross MD, Al-Nahhas A, *et al.* Nuclear medicine procedures in the diagnosis and therapy of medullary thyroid carcinoma. *Biomed Pharmacother* 2008; **62**:139–146.
9 Jacobson AF, Deng H, Lombard J, Lessig HJ, Black RR. 123I-metaiodobenzylguanidine scintigraphy for the detection of neuroblastoma and pheochromocytoma: results of a meta-analysis. *J Clin Endocrinol Metab* 2010; **95**:2596–2606.
10 Furuta N, Kiyota H, Yoshigoe F, Hasegawa N, Ohishi Y. Diagnosis of pheochromocytoma using [123I]-compared with [131I]-metaiodobenzylguanidine scintigraphy. *Int J Urol* 1999; **6**:119–124.
11 Koopmans KP, Neels ON, Kema IP, Elsinga PH, Links TP, de Vries EG, *et al.* Molecular imaging in neuroendocrine tumors: molecular uptake mechanisms and clinical results. *Crit Rev Oncol Hematol* 2009; **71**: 199–213.
12 Adler JT, Meyer-Rochow GY, Chen H, Benn DE, Robinson BG, Sippel RS, *et al.* Pheochromocytoma: current approaches and future directions. *Oncologist* 2008; **13**:779–793.
13 Bombardieri E, Giammarile F, Aktolun C, Baum RP, Bischof Delaloye A, Maffioli L, *et al.* 131I/123I-metaiodobenzylguanidine (mIBG) scintigraphy: procedure guidelines for tumour imaging. *Eur J Nucl Med Mol Imaging* 2010; **37**:2436–2446.
14 Taggart DR, Han MM, Quach A, Groshen S, Ye W, Villablanca JG, *et al.* Comparison of iodine-123 metaiodobenzylguanidine (MIBG) scan and [18F]fluorodeoxyglucose positron emission tomography to evaluate response after iodine-131 MIBG therapy for relapsed neuroblastoma. *J Clin Oncol* 2009; **27**:5343–5349.
15 Sharp SE, Shulkin BL, Gelfand MJ, Salisbury S, Furman WL. 123I-MIBG scintigraphy and 18F-FDG PET in neuroblastoma. *J Nucl Med* 2009; **50**:1237–1243.
16 Papathanasiou ND, Gaze MN, Sullivan K, Aldridge M, Waddington W, Almuhaideb A, *et al.* 18F-FDG PET/CT and 123I-metaiodobenzylguanidine imaging in high-risk neuroblastoma: diagnostic comparison and survival analysis. *J Nucl Med* 2011; **52**:519–525.
17 Timmers HJ, Chen CC, Carrasquillo JA, Whatley M, Ling A, Havekes B, *et al.* Comparison of 18F-fluoro-L-DOPA, 18F-fluoro-deoxyglucose, and 18F-fluorodopamine PET and 123I-MIBG scintigraphy in the localization of pheochromocytoma and paraganglioma. *J Clin Endocrinol Metab* 2009; **94**:4757–4767.
18 Kroiss A, Putzer D, Uprimny C, Decristoforo C, Gabriel M, Santner W, *et al.* Functional imaging in phaeochromocytoma and neuroblastoma with 68Ga-DOTA-Tyr 3-octreotide positron emission tomography and 123I-metaiodobenzylguanidine. *Eur J Nucl Med Mol Imaging* 2011; **38**:865–873.
19 Campbell L, Mouratidis B, Sullivan P. Improved detection of disseminated pheochromocytoma using post therapy I-131 MIBG scanning. *Clin Nucl Med* 1996; **21**:960–963.
20 Fukuoka M, Taki J, Mochizuki T, Kinuya S. Comparison of diagnostic value of I-123 MIBG and high-dose I-131 MIBG scintigraphy including incremental value of SPECT/CT over planar image in patients with malignant pheochromocytoma/paraganglioma and neuroblastoma. *Clin Nucl Med* 2011; **36**:1–7.
21 Rufini V, Calcagni ML, Baum RP. Imaging of neuroendocrine tumors. *Semin Nucl Med* 2006; **36**:228–247.
22 Ali N, Sebastian C, Foley RR, Murray I, Canizales AL, Jenkins PJ, *et al.* The management of differentiated thyroid cancer using ^{123}I for imaging to assess the need for ^{131}I therapy. *Nucl Med Commun* 2006; **27**:165–169.
23 Iwano S, Kato K, Nihashi T, Ito S, Tachi Y, Naganawa S. Comparisons of I-123 diagnostic and I-131 post-treatment scans for detecting residual thyroid tissue and metastases of differentiated thyroid cancer. *Ann Nucl Med* 2009; **23**:777–782.
24 Donahue KP, Shah NP, Lee SL, Oates ME. Initial staging of differentiated thyroid carcinoma: continued utility of posttherapy 131I whole-body scintigraphy. *Radiology* 2008; **246**:887–894.
25 Gedik GK, Hoefnagel CA, Bais E, Olmos RA. 131I-MIBG therapy in metastatic phaeochromocytoma and paraganglioma. *Eur J Nucl Med Mol Imaging* 2008; **35**:725–733.
26 Safford SD, Coleman RE, Gockerman JP, Moore J, Feldman JM, Leight GS Jr., *et al.* Iodine-131 metaiodobenzylguanidine is an effective treatment for malignant pheochromocytoma and paraganglioma. Surgery. 2003; **134**:956–962; discussion 962-963.
27 Fitzgerald PA, Goldsby RE, Huberty JP, Price DC, Hawkins RA, Veatch JJ, *et al.* Malignant pheochromocytomas and paragangliomas: a phase II study of therapy with high-dose 131I-metaiodobenzylguanidine (131I-MIBG). *Ann N Y Acad Sci* 2006; **1073**:465–490.
28 Olivier P, Colarinha P, Fettich J, Fischer S, Frokier J, Giammarile F, *et al.* Guidelines for radioiodinated MIBG scintigraphy in children. *Eur J Nucl Med Mol Imaging* 2003; **30**:B45–B50.

Comparison of Diagnostic Value of I-123 MIBG and High-Dose I-131 MIBG Scintigraphy Including Incremental Value of SPECT/CT Over Planar Image in Patients With Malignant Pheochromocytoma/Paraganglioma and Neuroblastoma

Makoto Fukuoka, MD, Junichi Taki, MD, PhD,* Takafumi Mochizuki, MD, PhD,* and Seigo Kinuya, MD, PhD†*

Purpose: To compare lesion detectability of I-123 MIBG scintigraphy with that of high-dose I-131 MIBG and to evaluate incremental benefit of SPECT/CT over planar image for the detection and localization of the lesions in patients with I-131 MIBG therapy for malignant pheochromocytoma/paraganglioma and neuroblastoma.

Materials and Methods: We retrospectively investigated 16 patients with malignant pheochromocytoma/paraganglioma and neuroblastoma, who were referred for I-131 MIBG therapy. We investigated the lesion detectability in 10 pairs of I-123 and high-dose I-131 MIBG studies of the same patient, obtained within 2 weeks. In 31 studies of I-123 MIBG scintigraphy in 16 patients and 17 studies of high-dose I-131 MIBG scintigraphy in 12 patients, we compared planar and SPECT/CT images for the lesion detectability and localization.

Results: The number of lesions detected by I-123 MIBG planer image and SPECT/CT and high-dose planer I-131 MIBG and SPECT/CT were 3.0 and 3.7, 7.3 and 7.7 per study, respectively. SPECT/CT images provided additional diagnostic information over planar images in 25 studies (81%) of 12 patients (75%) in I-123 MIBG scintigraphy and in 9 studies (53%) of 9 patients (75%) in high-dose I-131 MIBG scintigraphy.

Conclusion: Post-therapy high-dose I-131 MIBG scintigraphy is superior to I-123 MIBG scintigraphy in lesion detectability even in comparison with I-123 MIBG SPECT/CT images and high-dose I-131 MIBG planar images in patients with malignant neuroendocrine tumors. SPECT/CT images are helpful for accurate identification of anatomic localization compared with planar images.

Key Words: malignant neuroendocrine tumor, I-123-MIB, I-131 MIBG, SPECT/CT

(*Clin Nucl Med* 2011;36: 1–7)

Metaiodobenzylguanidine (MIBG) is a guanethidine derivative resembling the neurotransmitter norepinephrine in chemical structure. Therefore, showing the similar performance as norepinephrine, MIBG is taken up by the norepinephrine transporter (uptake 1) or passive diffusion, and stored in chromaffin deposit granules or neurosecretory granules in tissues derived from sympathetic nervous system.[1,2] In this mechanism, MIBG accumulates in tumors originated from neural crests.

Received for publication March 26, 2010; accepted July 6, 2010.
From the *Department of Nuclear Medicine, Kanazawa University Hospital, Kanazawa, Japan; and †Department of Biotracer Medicine, Kanazawa University Graduate School of Medical Sciences, Kanazawa, Japan.
There are no financial disclosures from any authors.
Reprints: Junichi Taki, MD, PhD, Department of Nuclear Medicine, Kanazawa University Hospital, 13–1 Takara-machi, Kanazawa, 920–8640, Japan. E-mail: taki@med.kanazawa-u.ac.jp.

ISSN: 0363-9762/11/3601-0001

Pheochromocytoma/paraganglioma and neuroblastoma are the representative neuroendocrine neoplasms showing intense MIBG accumulation. Pheochromocytoma/paraganglioma is a rare tumor which arises from chromaffin cells of the adrenal medulla/extra-adrenal sympathetic ganglia. It is reported that approximately 10% of pheochromocytoma and up to 40% of paraganglioma are malignant.[3,4] Neuroblastoma is one of the most common tumor derived from the embryonal sympathetic nervous system in children. Approximately 30% of neuroblastoma originate from the adrenal medulla and the rest arise from anywhere extra-adrenal sympathetic nervous system.[5,6] Malignant pheochromocytoma/paraganglioma and neuroblastoma usually matastasize to the bones, liver, lung, and lymph nodes in early times.

Since I-131 labeled MIBG scintigraphy for pheochromocytoma was reported in 1981, I-131 and I-123 labeled MIBG scintigraphy has been widely used as an excellent functional imaging modality for detection of the lesions in patients with neuroendocrine tumors.[7–9] MIBG scintigraphy is also useful for detection of the recurrent or metastatic lesions in patients with malignant pheochromocytoma/paraganglioma and neuroblastoma, although it is reported that the sensitivity in detecting extra-adrenal or malignant tumors is less than that in adrenal or benign tumors.[10–13] In the image quality and lesion detectability, I-123 MIBG image is superior to I-131 MIBG with diagnostic low radioactive dose,[14,15] because the γ-ray energy of I-123 (159 keV) is more suitable for scintigraphy compared with that of I-131 (364 keV). In addition to low-dose I-123 MIBG imaging, high-dose I-131 MIBG imaging is possible in patients who underwent I-131 MIBG internal radiation therapy, which is a precious option of the systemic treatments especially in those patients who have irresectable or multiple metastatic lesions. A case report demonstrated that post-therapeutic high-dose I-131 MIBG scintigraphy detected more lesions than low-dose diagnostic I-123 MIBG scintigraphy in a patient underwent I-131 MIBG therapy.[16] Similar findings were observed in the diagnostic I-123 and high-dose post-treatment I-131 scintigraphy in thyroid cancer.[17]

Accurate identification of anatomic localization of the lesions is important to perform I-131 MIBG therapy safely. However, it is difficult to identify accurate anatomic localization of the lesions in the conventional planar image. Comparing SPECT with CT or MRI image side-by-side or SPECT- CT or MRI fusion image by use of software has contributed to the precise definition of the localization to some degree.[18–20] Recently, integrated SPECT/CT fusion system which acquires the dual modality in the same session provides more additional information for characterization and localization of the lesions in various neuroendocrine tumors.[21–26]

The aim of this study was to compare lesion detectability of the I-123 MIBG scintigraphy with that of high-dose I-131 MIBG scintigraphy and to evaluate incremental benefit of I-123 MIBG and high-dose I-131 MIBG SPECT/CT over conventional planar image

TABLE 1. Clinical Characteristics of Patients

Patient Number	Age	Sex	Diagnosis	No. I-131 MIBG Therapy	Cumulative Dose of I-131MIBG (mCi)	No. I-123 MIBG Scintigraphy	No. High-Dose I-131 MIBG Scintigraphy
1	69	M	pheo	2	400	3	2
2	37	F	pheo	2	400	3	2
3	60	F	pheo	2	400	3	2
4	63	M	para	1	200	3	1
5	66	M	pheo	3	600	2	0
6	54	F	para	1	200	3	1
7	47	M	pheo	4	1360	2	1
8	36	M	para	0	0	1	0
9	7	F	neuro	1	100	1	1
10	8	M	neuro	0	0	1	0
11	13	F	neuro	3	600	3	3
12	7	M	neuro	1	300	1	1
13	11	F	neuro	1	400	1	1
14	7	F	neuro	1	300	1	1
15	8	F	neuro	1	100	2	0
16	10	M	neuro	1	400	1	1

MIBG indicates metaiodobenzylguanidine; pheo, malignant pheochromocytoma; para, malignant paraganglioma; neuro, neuroblastoma.

TABLE 2. The Number of Detected Lesions in 10 Pairs of I-123 and High-Dose I-131 MIBG Scinitgraphies Performed Within 2 Weeks in the Same Patient

Patient Number	I-123 MIBG Planar Image	I-123 MIBG SPECT/CT	I-131 MIBG Planar Image	I-131 MIBG SPECT/CT
1	0	1	1	1
2	6	6	6	6
3	1	2	4	6
4	1	1	1	1
5	1	3	15	15
6	1	2	8	9
7	2	2	7	7
8	0	0	3	2
9	15	15	15	17
10	3	5	13	13
Total	30	37	73	77

MIBG indicates metaiodobenzylguanidine.

for the detection and localization of the lesions in patients who underwent I-131 MIBG therapy for malignant pheochromocytoma/paraganglioma and neuroblastoma.

MATERIALS AND METHODS

Patients

We retrospectively investigated 16 patients with malignant pheochromocytoma/paraganglioma and neuroblastoma, who were referred for I-131 MIBG therapy in our institute and underwent I-123 MIBG (111 MBq [3 mCi]) and/or high-dose I-131 MIBG (3.7–14.8 GBq [100–400 mCi]) scintigraphy from June 2008 to August 2009 (5 males and 3 females with malignant pheochromocytoma/paraganglioma, mean age 54 years [range, 36–69 years]; 3 males and 5 females with neuroblastoma, mean age 8.8 years [range, 7–13 years] (Table 1). Thirty-one studies of I-123 MIBG scintigraphy were obtained in 16 patients and 17 studies of high-dose I-131 MIBG scintigraphy were acquired in 12 patients.

I-123 MIBG Scintigraphy With Diagnostic Low-Radioactive Dose

I-123 MIBG scintigraphy was performed after intravenous injection of 111 MBq (3 mCi) of radiopharmaceutical for all patients, using a dual-head gamma camera equipped with a low-intermediate energy collimator and a 5/8 inch NaI crystal, which was combined to a low-dose spiral CT by the same gantry (Symbia, Siemens Medical Solutions). Whole-body planar images were acquired at 6 and 24 hours after I-123 MIBG injection at scanning speeds of 15 cm/min. Following planar imaging after 6 hours of tracer injection, SPECT images were obtained to cover the areas suspected of abnormal tracer accumulations in whole-body planar images. SPECT data were acquired from 60 projections (20 seconds per view) with 128 × 128 matrix and reconstructed using a 3-dimensional iterative algorithm, ordered-subsets expectation maximization. As soon as SPECT data acquisition was finished, CT transmission scans for tomography were performed. SPECT and CT data were analyzed and coregistered using an e-soft workstation.

I-131 MIBG Therapy and Scintigraphy With Post-Therapy High-Radioactive Dose

I-131 MIBG therapy was administered to the patients who were considered to have beneficial therapeutic effects through the findings of pretherapy I-123 MIBG scintigraphy. 3.7–14.8 GBq (100–400 mCi) of I-131 MIBG was injected intravenously through fixed peripheral venous lines for about an hour, using lead-shielded infusion pump. Vital signs were monitored for more than 6 hours from the beginning of I-131 MIBG administration. I-131 MIBG planar and SPECT/CT images were acquired 3 days later in the same way as I-123 MIBG scintigraphy, except for the use of collimator (high-energy).

Image Interpretation

At first, I-123 or I-131 MIBG planar images were evaluated by 2 experienced nuclear medicine physicians, who were blinded to the findings of the other imaging modalities. They were asked to interpret all focal uptakes, except for physiological accumulation, as

TABLE 3. Number of Lesions in I-123 MIBG Imaging

Study Number	Diagnosis	No. Lesions in Planar Image	No. Lesions in SPECT/CT	No. Newly Detected Lesions in SPECT/CT	No. Lesions Turned to be Negative in SPECT/CT	No. Lesions Modified Anatomical Localization by SPECT/CT
1	neuro	0	0	0	0	0
2	para	1	2	1	0	1
3	pheo	2	3	1	0	0
4	neuro	2	3	1	0	1
5	pheo	1	1	0	0	0
6	pheo	6	6	0	0	2
7	pheo	3	4	1	0	0
8	pheo	0	1	1	0	0
9	neuro	1	1	0	0	0
10	para	2	3	1	0	1
11	para	25	25	0	0	2
12	neuro	3	5	2	0	0
13	neuro	0	0	0	0	0
14	neuro	23	18	0	5	3
15	neuro	1	2	1	0	1
16	neuro	1	3	2	0	0
17	para	1	2	1	0	1
18	pheo	2	2	0	0	1
19	neuro	1	1	0	0	0
20	pheo	2	2	0	0	0
21	pheo	1	3	2	0	0
22	pheo	3	3	0	0	0
23	pheo	1	1	0	0	1
24	para	16	16	0	0	2
25	neuro	2	2	1	1	0
26	pheo	3	4	1	0	0
27	pheo	1	1	0	0	0
28	pheo	3	3	0	0	1
29	pheo	1	1	1	1	0
30	para	22	22	0	0	3
31	neuro	15	15	1	1	1
Total		145	155	18	8	21

MIBG indicates metaiodobenzylguanidine; pheo, malignant pheochromocytoma; para, malignant paraganglioma; neuro, neuroblastoma.

abnormal lesions and to define their anatomic locations. Diffuse accumulation at nasal cavity, salivary glands, thyroid, myocardium, liver, and bladder was considered as physiological uptake. When their interpretations were discordant, consensus was obtained after a conference. Then, SPECT/CT images were assessed by them independently with planar images and they were required to re-evaluate the anatomic location of the lesions found in planar images and indicate new lesions. The findings suspected of metastasis in CT images alone were not included in new lesions if they did not accompany MIBG accumulation. Consensus was acquired in the same way as planar image if their interpretation was discordant.

Data Analysis

In comparison of diagnostic value of I-123 MIBG and high-dose I-131 MIBG scintigraphy, we investigated the difference of the number of detected lesions in 10 pairs of I-123 and high-dose I-131 MIBG studies of the same patient that were obtained within 2 weeks. In the evaluation of incremental diagnostic value of SPECT/CT images over planar images with I-123 MIBG and high-dose I-131 MIBG, we performed comparative analysis between planar and SPECT/CT images in all patients.

RESULTS

In I-123 MIBG scintigraphy, a total of 145 and 155 abnormal uptakes were pointed out in planar and SPECT/CT images, respectively, in 31 studies of 16 patients. In high-dose I-131 MIBG scintigraphy, a total of 136 and 140 abnormal uptakes were pointed out in planar and SPECT/CT images, respectively, in 17 studies of 12 patients.

In comparison of all 10 pairs of I-123 and high-dose I-131 MIBG studies in the same patient that were obtained within 2 weeks, the lesions detected by I-123 MIBG scintigraphy were 3.0/study in planar image, 3.7/study in SPECT/CT image; and the lesions detected by high-dose I-131 MIBG scintigraphy were 7.3/study in planar image, 7.7/study in SPECT/CT images. The number of detected lesions is summarized in Table 2.

In all I-123 MIBG SPECT/CT images, 18 new lesions, which had not been pointed out in planar images, were detected in 14 studies (45.2%) of 11 patients (68.8%), but 8 lesions which had been recognized in planar images became undetectable in 4 studies (12.9%) of 2 patients (12.5%). Anatomic locations of 21 lesions in planar image were modified after analysis of SPECT/CT images in 14 studies (45.2%) of 10 patients (62.5%). As a whole, SPECT/CT

TABLE 4. Number of Lesions in High-Dose I-131 MIBG Imaging

Study Number	Diagnosis	No. Lesions in Planar Image	No. Lesions in SPECT/CT	No. Newly Detected Lesions in SPECT/CT	No. Lesions Turned to be Negative in SPECT/CT	No. Lesions Modified Anatomical Localization by SPECT/CT
1	pheo	2	2	0	0	0
2	pheo	1	1	0	0	0
3	pheo	6	6	0	0	0
4	pheo	5	6	1	0	0
5	para	4	6	2	0	3
6	para	35	35	0	0	3
7	pheo	2	2	0	0	0
8	pheo	3	3	0	0	0
9	pheo	7	7	0	0	1
10	neuro	1	1	0	0	0
11	neuro	15	15	0	0	1
12	neuro	9	8	0	1	0
13	neuro	8	9	1	0	2
14	neuro	7	7	0	0	0
15	neuro	3	2	0	1	1
16	neuro	15	17	2	0	5
17	neuro	13	13	0	0	1
Total		136	140	6	2	17

MIBG indicates metaiodobenzylguanidine; pheo, malignant pheochromocytoma; para, malignant paraganglioma; neuro, neuroblastoma.

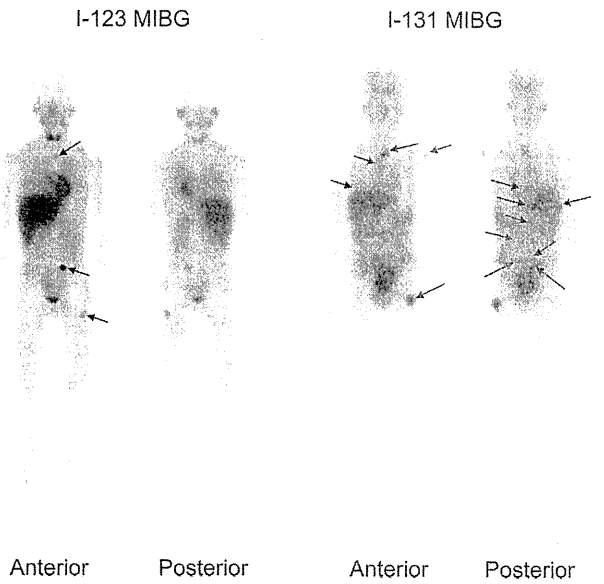

FIGURE 1. A 10-year-old boy with neuroblastoma underwent 14.8 GBq (400 mCi) of I-131 MIBG therapy. In the planar image with diagnostic I-123 MIBG, only 3 abnormal uptakes were detected in the upper mediastinum, left lower abdomen, and left thigh. In the planar image with therapeutic high-dose I-131 MIBG, total of 13 abnormal uptakes were detected in the left shoulder, mediastinum, vertebrae, upper and lower abdomen, and in the left thigh.

images provided additional diagnostic information over planar images in 25 studies (80.6%) of 12 patients (75.0%). The number of the lesions detected in I-123 MIBG planar and SPECT/CT imaging is summarized in Table 3.

In high-dose I-131 MIBG SPECT/CT images, 6 new lesions were detected in 4 studies (23.5%) of 4 patients (33.3%), but 2 lesions which had been recognized in planar images became obscure in 2 studies (11.8%) of 2 patients (16.7%). Anatomic locations of 17 lesions were altered after the evaluation of SPECT/CT images in 8 studies (47.1%) of 8 patients (66.7%). As a whole, SPECT/CT images provided additional diagnostic information in 9 studies (52.9%) of 9 patients (75.0%) over planar images. The number of the lesions in high-dose I-131 MIBG planar and SPECT/CT imaging is summarized in Table 4.

Most of the new lesions detected in SPECT/CT were located near the physiological uptake or were overlapped with the physio-

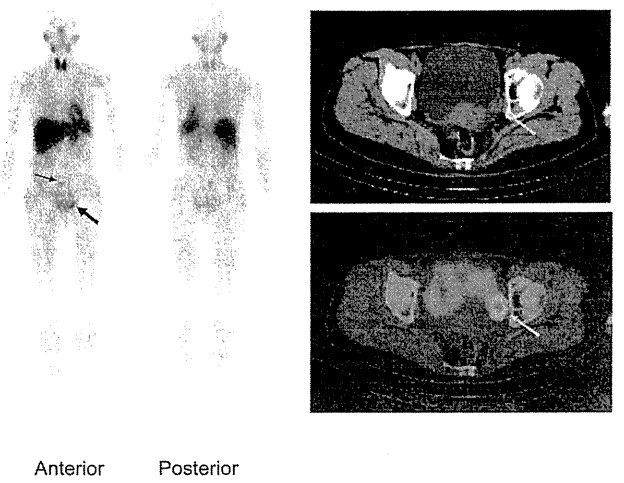

FIGURE 2. A 54-year-old woman with malignant paraganglioma underwent diagnostic I-123 MIBG scintigraphy. In the planar image, it is easy to point out the abnormal accumulation in the lower abdomen (narrow arrow), however, it is difficult to detect the abnormal uptake beside the bladder (wide arrow) because of physiological accumulation in the bladder. In the SPECT/CT, it is easy to detect the abnormal MIBG accumulation corresponding to the nodular lesion in the left side of the bladder.

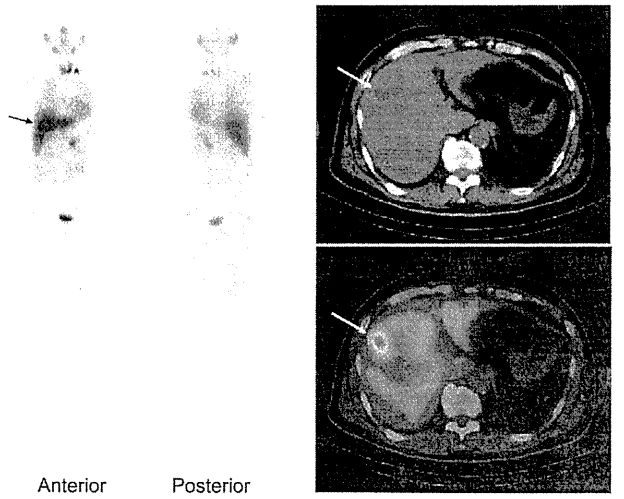

FIGURE 3. A 47-year-old woman with malignant pheochromocytoma underwent diagnostic low-dose I-123 MIBG scintigraphy. In the planar image, it is difficult to determine whether the abnormal uptake in the right upper abdomen exists in the right rib or in the liver. In the SPECT/CT, it is proved that the abnormal accumulation exists in the liver.

logical accumulation. In I-123 MIBG SPECT/CT images, 10 of 18 newly detected lesions by SPECT/CT were overlapped with the physiological accumulation and 1 new lesion was detected as a lymph node, 4 were in bones, and 3 were in lungs. In high-dose I-131 MIBG SPECT/CT images, 4 of 6 newly detected lesions were overlapped with the physiological accumulation and other one lesion was detected as a lymph node and another one was in a bone. All of the lesions turned to be negative in SPECT/CT were suspected to be located in bones in planar images.

The representative comparative planar images with I-123 MIBG and high-dose I-131 MIBG of a 10-year-old male patient with neuroblastoma are shown in Figure 1. A representative case with beneficial I-123 MIBG SPECT/CT over planar image for the detection of the lesion is shown in Figure 2. A case with beneficial SPECT/CT over planar image for the localization of the abnormal uptake is shown in Figure 3.

DISCUSSION

I-131 MIBG internal radiation therapy has become popular as a systemic therapy for patients with malignant neuroendocrine tumors such as malignant pheochromocytoma, malignant paraganglioma, and neuroblastoma with metastatic lesions[27–30] in addition to chemotherapy represented by combined regimen of cyclophosphamide, vincristine, and dacarbazine.[31] For the indication of I-131 MIBG therapy, it is essential to confirm MIBG accumulation to the metastatic lesions and to rule out MIBG accumulation to high-risk sites such as the lesion compressing spinal cord. In our institute,

indication of I-131 MIBG therapy is usually determined based on the results of I-123 MIBG scintigraphy including SPECT/CT to identify accurate anatomic localization of the lesions, because image quality of I-123 MIBG scintigraphy is generally superior to diagnostic low-dose I-131 MIBG scintigraphy.[14,15] After I-131 MIBG therapy, I-131 MIBG imaging might be recommended in order to confirm the lesions with MIBG accumulation. In this study; more than 2 times lesions were detected in high-dose I-131 MIBG scintigraphy than in diagnostic I-123 MIBG scintigraphy. Even an I-123 MIBG SPECT/CT was inferior to planar high-dose I-131 MIBG image in lesion detectability (3.7 vs. 7.3 lesions/study, respectively). Since high-dose I-131 MIBG scintigraphy have great diagnostic value in the detection of the lesions, it is believed that I-131 MIBG scintigraphy after I-131 MIBG therapy is essential for the management of patients.

Recently, many studies investigated the incremental value of SPECT/CT over planar image in various tumors. Even-Sapir et al reported that SPECT/CT improved image interpretation by providing a better anatomic localization of SPECT-detected lesions in 41% of the patients with known or suspected endocrine tumor and detected unsuspected bone involvement in 15% of the patients.[21] Rozovsky et al investigated added value of SPECT/CT over the correlation of I-123 MIBG scintigraphy and diagnostic CT in neuroblastoma and pheochromocytoma and reported that SPECT/CT provided additional information in 53% of all cases.[26] In various type of tumor scans, Roach et al reported that SPECT/CT modified the interpretation with planar/SPECT alone in 56% of the cases.[32] Chen et al reported that, in patients with differentiated thyroid carcinoma, precise localization and characterization of I-131-avid foci were achieved through I-131 SPECT/CT over planar image in 69 (85.2%) and 67 (82.7%) of the 81 foci, respectively, and uncommon metastatic lesions were found in 9 (13.6%) of 66 patients with regard to SPECT/CT fusion images.[33] In our study, unknown lesions in planar images were detected by SPECT/CT images in 45.2% of studies and 68.8% of patients and anatomic locations of the lesions were modified after analysis of SPECT/CT in 45.2% of studies and 62.5% of patients in I-123 MIBG scintigraphy. In high-dose I-131 MIBG scintigraphy, unknown lesions in planar images were detected by SPECT/CT in 23.5% of studies and 33.3% of patients and anatomic locations of the lesions were altered after analysis of SPECT/CT in 47.1% of studies and 66.7% of patients. As a whole, SPECT/CT images provided additional diagnostic information in 80.6% of studies, 75.0% of patients and 52.9% of studies, 75.0% of patients over planar images in I-123 MIBG scintigraphy and high-dose I-131 MIBG scintigraphy, respectively. The detection rate of the new lesions by SPECT/CT was higher in I-123 MIBG scintigraphy than in high-dose I-131 MIBG scintigraphy. It is thought that signal-to-noise ratio is high enough to be identified in planar image when high dose is administered. There were no apparent differences in the rate of alteration of anatomic location of the lesions between diagnostic I-123 MIBG and high-dose I-131 MIBG images.

A few lesions found in planar images became undetectable in SPECT/CT images in both I-123 MIBG and I-131 MIBG. Because all lesions showed weak uptake, low lesion counts of each projection image might not permit to develop tomographic image.

CONCLUSIONS

Post-therapy high-dose I-131 MIBG scintigraphy is superior to diagnostic I-123 MIBG scintigraphy for lesion detectability even in comparison with I-123 MIBG SPECT/CT images and high-dose I-131 MIBG planar images in patients with malignant neuroendocrine tumor. SPECT/CT images are helpful for the detection of the new lesions and accurate identification of anatomic localization compared with planar images. SPECT/CT imaging is especially useful for the detection of the lesions near or overlapping physiological accumulation compared with planar images.

REFERENCES

1. Jaques S, Tobes MC, Sisson JC. Sodium dependency of uptake of norepinephrine and m-iodobenzylguanidine into cultured human pheochromocytoma cells: evidence for uptake-one. *Cancer Res.* 1987;47:3920–3928.
2. Gasnier B, Roisin MP, Scherman D, et al. Uptake of metaiodobenzylguanidine by bovine chromaffin granule membranes. *Mol Pharmacol.* 1986;29:275–280.
3. Edström Elder E, Hjelm Skog AL, Höög A, et al. The management of benign and malignant pheochromocytoma and abdominal paraganglioma. *Eur J Surg Oncol.* 2003;29:278–283.
4. Whalen RK, Althausen AF, Daniels GH. Extra-adrenal pheochromocytoma. *J Urol.* 1992;147:1–10.
5. Lonergan GF, Schwab CM, Suarez ES, et al. From the archives of the AFIP neuroblastoma, ganglioneuroblastoma, and ganglioneuroma: radiologic-pathologic correlation. *Radiographics.* 2002;29:911–934.
6. Papaioannou G, McHugh K. Neuroblastoma in childhood: review and radiological findings. *Cancer Imaging.* 2005;5:116–127.
7. Sisson JC, Frager MS, Valk TW, et al. Scintigraphic localization of pheochromocytoma. *N Engl J Med.* 1981;305:12–17.
8. Shapiro B, Copp JE, Sisson JC, et al. Iodine-131 metaiodobenzylguanidine for the locating of suspected pheochromocytoma: experience in 400 cases. *J Nucl Med.* 1985;26:576–585.
9. Boubaker A, Bischof Delaloye A. MIBG scintigraphy for the diagnosis and follow-up of children with neuroblastoma. *Q J Nucl Med Mol Imaging.* 2008;52:388–402.
10. van der Harst E, de Herder WW, Bruining HA, et al. [I-123] metaiodobenzylguanidine and [In-111]octreotide uptake in benign and malignant pheochromocytomas. *J Clin Endocrinol Metab.* 2001;86:685–693.
11. van der Horst-Schrivers AN, Jager PL, Boezen HM, et al. Iodine-123 metaiodobenzylguanidine scintigraphy in localising phaeochromocytomas—experience and meta-analysis. *Anticancer Res.* 2006;26:1599–1604.
12. Bhatia KS, Ismail MM, Sahdev A, et al. 123I-metaiodobenzylguanidine (MIBG) scintigraphy for the detection of adrenal and extra-adrenal phaeochromocytomas: CT and MRI correlation. *Clin Endocrinol (Oxf).* 2008;69:181–188.
13. Wiseman GA, Pacak K, O'Dorisio MS, et al. Usefulness of I-123 MIBG scintigraphy in the evaluation of patients with known or suspected primary or metastatic pheochromocytoma or paraganglioma: results from a prospective multicenter trial. *J Nucl Med.* 2009;50:1448–1454.
14. Shulkin BL, Shapiro B, Francis IR, et al. Primary extra-adrenal pheochromocytoma: positive I-123 MIBG imaging with negative I-131 MIBG imaging. *Clin Nucl Med.* 1986;11:851–854.
15. Lynn MD, Shapiro B, Sisson JC, et al. Pheochromocytoma and the normal adrenal medulla: improved visualization with I-123 MIBG scintigraphy. *Radiology.* 1985;156:789–792.
16. Campbell L, Mouratidis B, Sullivan P. Improved detection of disseminated pheochromocytoma using post therapy I-131 MIBG scanning. *Clin Nucl Med.* 1996;21:960–963.
17. Iwano S, Kato K, Nihashi T, et al. Comparisons of I-123 diagnostic and I-131 post-treatment scans for detecting residual thyroid tissue and metastases of differentiated thyroid cancer. *Ann Nucl Med.* 2009;23:777–782.
18. Weber DA, Ivanovic M. Correlative image registration. *Semin Nucl Med.* 1994;24:311–323.
19. Pérault C, Schvartz C, Wampach H, et al. Thoracic and abdominal SPECT-CT image fusion without external markers in endocrine carcinomas. *J Nucl Med.* 1997;38:1234–1242.
20. Hutton BF, Braun M, Thurfjell L, et al. Image registration: an essential tool for nuclear medicine. *Eur J Nucl Med.* 2002;29:559–577.
21. Even-Sapir E, Keidar Z, Sachs J, et al. The new technology of combined transmission and emission tomography in evaluation of endocrine neoplasms. *J Nucl Med.* 2001;42:998–1004.
22. Pfannenberg AC, Eschmann SM, Horger M, et al. Benefit of anatomical-functional image fusion in the diagnostic work-up of neuroendocrine neoplasms. *Eur J Nucl Med Mol Imaging.* 2003;30:835–843.
23. Schillaci O. Functional-anatomical image fusion in neuroendocrine tumors. *Cancer Biother Radiopharm.* 2004;19:129–134.
24. Morcila PP, Duarte LH, Vieira F, et al. Value of SPECT/CT image fusion in the assessment of neuroendocrine tumours with In-111 pentetreotide scintigraphy. *Rev Esp Med Nucl.* 2005;24:14–18.

25. Anthauer H, Denecke T, Rohlfing T, et al. Value of image fusion using single photon emission computed tomography with integrated low dose computed tomography in comparison with a retrospective voxel-based method in neuroendocrine tumours. *Eur Radiol*. 2005;15:1456–1462.
26. Rozovsky K, Koplewitz B, Krausz Y, et al. Added value of SPECT/CT for correlation of MIBG scintigraphy and diagnostic CT in neuroblastoma and pheochromocytoma. *AJR*. 2008;190:1085–1090.
27. Sisson JC, Shapiro B, Beierwaltes WH, et al. Radiopharmaceutical treatment of malignant pheochromocytoma. *J Nucl Med*. 1984;24:197–206.
28. Gedik GK, Hoefnagel CA, Bais E, et al. I-131 MIBG therapy in metastatic phaeochromocytoma and paraganglioma. *Eur J Nucl Med Mol Imaging*. 2008;35:725–733.
29. Gonias S, Goldsby R, Matthay KK, et al. Phase II study of high-dose [I-131]metaiodobenzylguanidine therapy for patients with metastatic pheochromocytoma and paraganglioma. *J Clin Oncol*. 2009;27:4162–4168.
30. DuBois SG, Matthay KK. Radiolabeled metaiodobenzylguanidine for the treatment of neuroblastoma. *Nucl Med Biol*. 2008;35:35–48.
31. Scholz T, Eisenhofer G, Pacak K, et al. Clinical review: current treatment of malignant pheochromocytoma. *J Clin Endocrinol Metab*. 2007;92:1217–1225.
32. Roach PJ, Schembri GP, Ho Shon IA, et al. SPECT/CT imaging using a spital CT scanner for anatomical localization: impact on diagnostic accuracy and reporter confidence in clinical practice. *Nucl Med Commun*. 2006;27:977–987.
33. Chen L, Luo Q, Shen Y, et al. Incremental value of I-131 SPECT/CT in the management of patients with differentiated thyroid cancer. *J Nucl Med*. 2008;49:1952–1957.

Eur J Nucl Med Mol Imaging (2011) 38:1869–1875
DOI 10.1007/s00259-011-1872-3

ORIGINAL ARTICLE

Clinical significance of 2-[^{18}F]fluoro-2-deoxy-D-glucose positron emission tomography for the assessment of ^{131}I-metaiodobenzylguanidine therapy in malignant phaeochromocytoma

Azusa Nakazawa · Tetsuya Higuchi · Noboru Oriuchi · Yukiko Arisaka · Keigo Endo

Received: 16 March 2011 / Accepted: 17 June 2011 / Published online: 6 July 2011

Abstract
Purpose The aim of this study was to evaluate the significance of 2-[^{18}F]fluoro-2-deoxy-D-glucose (FDG) positron emission tomography (PET) in the assessment of the therapeutic response to ^{131}I-metaiodobenzylguanidine (MIBG) in malignant phaeochromocytoma.
Methods We reviewed the records of 11 patients (7 men and 4 women) with malignant phaeochromocytoma who underwent ^{131}I-MIBG therapy (100–200 mCi). ^{18}F-FDG PET and serum catecholamine assays were performed 3 months before and after the first dose of ^{131}I-MIBG. FDG uptake was evaluated in the observed lesions using the maximum standardised uptake value (SUV_{max}). The average SUV_{max} of all lesions (ASUV) was calculated. If more than five lesions were identified, the average SUV_{max} of the five highest SUV_{max} (ASUV5) was calculated. The ratio of pre- and post-therapy values was calculated for the highest SUV_{max} (rMSUV), ASUV (rASUV), ASUV5 (rASUV5), CT diameter (rCT) and serum catecholamine (rCA). Responder (R) and non-responder (NR) groups were defined after a clinical follow-up of at least 6 months according to changes in symptoms, CT, magnetic resonance imaging (MRI) and ^{123}I-MIBG scan.
Results Post-therapy evaluation revealed five R and six NR patients. The size of the target lesions was not significantly different before and after therapy ($p>0.05$). However, ASUV and ASUV5 were significantly lower in the R group (rASUV 0.64±0.18, rASUV5 0.68±0.17) compared to the NR group (rASUV 1.40±0.54, rASUV5 1.37±0.61) ($p<0.05$).
Conclusion ^{18}F-FDG PET can be potentially used to evaluate the response of malignant phaeochromocytoma to ^{131}I-MIBG therapy.

Keywords Phaeochromocytoma · 2-[^{18}F]Fluoro-2-deoxy-D-glucose (FDG) positron emission tomography (PET) · ^{131}I-metaiodobenzylguanidine (MIBG) · Malignant phaeochromocytoma · Radionuclide therapy

A. Nakazawa (✉) · T. Higuchi · N. Oriuchi · Y. Arisaka · K. Endo
Department of Diagnostic Radiology and Nuclear Medicine,
Gunma University Hospital,
3-39-22 Showa-machi,
Maebashi, Gunma 371-8511, Japan
e-mail: azusa-n@sea.sannet.ne.jp

Introduction

Phaeochromocytoma is a rare, catecholamine-producing tumour. It originates from chromaffin cells, mainly located in the adrenal medulla [1]. Although most phaeochromocytomas develop from the adrenal medulla, they may also derive from the extra-adrenal organs such as sympathetic paraganglia [2]. Phaeochromocytoma is diagnosed on the basis of symptoms of catecholamine excess, such as severe hypertension, sweating, headache and anxiety attacks [3].

The annual incidence of phaeochromocytoma is 1–4/10^6 population [1]. About 10% of these tumours metastasise. Classically, only metastasised tumours identified in the extra chromaffin tissue are considered malignant, for it is almost impossible to differentiate a benign from a malignant tumour only by histological criteria [4]. As a consequence, malignant phaeochromocytoma is not surgically curable. Moreover, surgically unresectable malignant phaeochromocytoma tumours have limited therapeutic options. These cases are currently treated mainly with combination chemotherapy including cyclophosphamide,

vincristine and dacarbazine (CVD). However, the chemotherapy frequently produces adverse events [5]. The 5-year survival rate of metastatic phaeochromocytoma has been reported to be less than 50% [6, 7]. Metaiodobenzylguanidine (MIBG) is a guanethidine analogue that is structurally similar to norepinephrine and accumulates in sympathomedullary tissues. ^{131}I-MIBG and ^{123}I-MIBG are commonly used in the diagnosis of phaeochromocytoma. A high dose of ^{131}I-MIBG has anti-tumour efficacy by emitting β-particles [8]. ^{131}I-MIBG was initially used in the treatment of phaeochromocytoma in 1983 [9]. The advantages of ^{131}I-MIBG therapy are effectiveness to both primary and metastatic lesions and relatively mild adverse events. The application of a ^{131}I-MIBG therapeutic protocol in phaeochromocytoma was established at a consensus meeting in Rome in 1991 [10].

Nevertheless, the assessment method for treatment with ^{131}I-MIBG is still controversial. In a retrospective study with 33 patients, Safford et al. reported that symptomatic and hormonal response to ^{131}I-MIBG therapy, but not reduction in tumour volume, was the best predictor of prolonged survival [11].

In contrast, Gonias et al. reported that MIBG scan or computed tomography/magnetic resonance imaging (CT/MRI), but not hormonal response, was predictive of overall survival (OS) after high-dose ^{131}I-MIBG therapy [12].

2-[^{18}F]Fluoro-2-deoxy-D-glucose (FDG) is a radiolabelled glucose analogue used for imaging of malignant tumours with high glucose metabolism. FDG has been applied to the diagnosis of phaeochromocytoma. Its usefulness for monitoring the efficiency of ^{131}I-MIBG therapy in malignant phaeochromocytoma has also been reported [13]. A comparative study between MIBG scan and FDG positron emission tomography (PET) revealed that FDG PET is able to detect a greater number of phaeochromocytoma lesions and metastases and that it may be used for the assessment of therapeutic effects [14]. In another comparative study by Menzel et al. [13], FDG PET revealed a significant decrease in standardised uptake value (SUV) after ^{131}I-MIBG therapy, while no significant volume reduction was detected by X-ray CT. Thus, determination of the SUV by FDG PET is expected to be a good alternative therapeutic assessment of the tumour which shows little change in size by CT/MRI [13]. Although several approaches have been performed, the appropriate procedure for therapeutic evaluation of ^{131}I-MIBG therapy in malignant phaeochromocytoma is still controversial.

In this study, we evaluated the efficacy of FDG PET for assessment of ^{131}I-MIBG therapy compared with X-ray CT and serum catecholamine levels in order to identify biomarkers for the treatment of malignant phaeochromocytoma.

Materials and methods

Patients and ^{131}I-MIBG therapy

We performed a retrospective review of 11 patients undergoing ^{131}I-MIBG therapy for malignant phaeochromocytoma for the first time from April 2006 to February 2010 in our institution. Patients with positive tracer uptake as assessed by ^{123}I-MIBG scan were selected for treatment. The dose of ^{131}I-MIBG was 100–200 mCi (3.7–7.4 GBq). We usually give two to three treatments of 100–200 mCi (3.7–7.4 GBq) with an at least 6-month interval. In this study, we analysed FDG PET and serum catecholamine assays which were performed 3 months before and after the first dose of ^{131}I-MIBG.

Patients with myelosuppression (haemoglobin <9.0 g/dl, white blood cell count <3,000 mm^{-3}, platelet count <100,000 mm^{-3}), patients who were pregnant or breast-feeding, and patients with an expected survival of less than 1 month or renal dysfunction with effective glomerular filtration rate <30 ml/min were excluded from this study.

To prevent solution (^{131}I-MIBG) leakage during administration, a central venous catheter was inserted through the right subclavian vein of all patients. ^{131}I-MIBG was infused intravenously for 30 min in a lead-shielded room with intravenous hydration.

Written informed consent was obtained from each patient before they were enrolled in the study, and the study protocol was approved by the Institutional Review Board. This study was conducted in accordance with the amended Helsinki Declaration. Our database and electronic charts were retrospectively reviewed to obtain follow-up data.

Imaging protocols

All patients underwent repeated FDG PET (eight scans) or PET/CT (three scans) 3 months before and after the first ^{131}I-MIBG therapy.

FDG was produced in our cyclotron facility. The patients were fasted for 6 h, and free of alcohol and caffeine for 12 h, before being given an intravenous injection of ^{18}F-FDG (5 MBq/kg). FDG PET/CT scans were performed with the Discovery STE (GE Healthcare, Waukesha, WI, USA) and Biograph 16 (Siemens Medical Solutions, Knoxville, TN, USA) scanners, with a 700-mm field of view (FOV) and slice thickness of 3.27 mm. The CT was acquired to correct PET transmission using the following parameters: 140 kV and 120–240 mAs to produce 128×128 matrix images. The patients were scanned in the arms-down position from head to thigh. Shallow breathing was advised to avoid motion artefacts and minimise misregistration of CT and PET images. Intravenous contrast material was not administered for CT scanning. After the CT scan, the PET

data were acquired, and acquisition time was 3 min per bed position. CT images were reconstructed by using the conventional filtered backprojection method. Axial full-width at half-maximum (FWHM) at 1 cm from the centre of the FOV was 6.3 mm. Intrinsic system sensitivity was 8.5 cps/kBq for three-dimensional acquisition.

Biochemical markers

Pre- and post-therapy assessment included the following markers of catecholamine metabolism: plasma norepinephrine, epinephrine and dopamine; and 24-h urine collection for fractionated catecholamines (norepinephrine, epinephrine and dopamine), metanephrine and normetanephrine. In this study, we adopted norepinephrine as a representative marker (upper reference limit <0.06 ng/ml in plasma).

Scan review and evaluation

FDG PET and PET/CT images were retrospectively reviewed by two experienced nuclear medicine physicians, who were blinded to all other imaging and clinical information, including biochemical markers. The SUV was used for image interpretation. FDG uptake of the observed lesions was evaluated using the maximum SUV (SUV_{max}), and tumour size was calculated on the basis of the sum of the longest diameter of the target lesions.

Statistical analysis

Responder (R) and non-responder (NR) patients were defined according to changes in symptoms, CT, MRI and ^{131}I-MIBG scan obtained after a period of at least 6 months of clinical follow-up. Symptoms included fatigue, flushing, sweat, diarrhoea, weight loss, etc. Symptomatic response was defined as either complete resolution or a subjective decrease in the intensity of symptoms, because the evaluation of these symptoms cannot help relying on a subjective evaluation excluding the one which can be measured by the numerical value. If a new lesion was detected by CT, MRI, PET or ^{131}I-MIBG scan after ^{131}I-MIBG therapy, the patient was classified into the NR group.

The average SUV_{max} of all lesions was defined as ASUV. The ratio of pre- and post-therapy ASUV was calculated (rASUV). If more than five lesions were identified by FDG PET, the average of the five highest SUV_{max} values was calculated (ASUV5). The ratio of pre- and post-therapy ASUV5 was also calculated (rASUV5). The lesion with the highest SUV_{max} was defined as MSUV. The ratio of pre- and post-therapy MSUV was calculated (rMSUV). In addition, the sum of the longest diameters of the lesions with the five highest SUV_{max} values (summed CT diameter) and the ratio of pre- and post-therapy summed CT diameter (rCT) were also calculated. For hormonal evaluation, the ratio of pre- and post-therapy serum catecholamine (rCA) was calculated.

The unpaired t test was used to evaluate the statistical significance of rASUV, rASUV5, rMSUV, rCT and rCA in the R and NR groups. Significance was set at $p<0.05$.

Results

The characteristics of the patients involved in the present study are summarised in Table 1. The patients were seven men and four women, aged 29–69 years [mean (SD) 49.4 (14.6) years]. Ten patients underwent surgery: three patients (27%) received radiotherapy, five patients (45%) received chemotherapy and two patients (18%) received both chemotherapy and radiotherapy before ^{131}I-MIBG administration. Of 11 patients, 8 (72%) had elevated serum catecholamine (norepinephrine) before ^{131}I-MIBG therapy, and 5 of 11 patients (45%) had elevated urinary catecholamine. The median dose of ^{131}I-MIBG was 7.4 GBq (3.7–7.4 GBq).

Table 1 Characteristics of patients

Patient	Age (years)/sex	Primary lesion	Previous treatment	Dose of ^{131}I-MIBG (mCi)
1	43/M	L adrenal	Op, chemo	100
2	34/F	L adrenal	Op	100
3	69/M	L neck	Op, chemo, RT	100
4	59/M	L adrenal	Op	150
5	51/M	L adrenal	Op, chemo, RT	150
6	29/F	Retroperitoneum	Op	200
7	39/F	L adrenal	Op, chemo	200
8	32/M	R adrenal	Op, RT	200
9	57/F	L adrenal	Op, chemo	200
10	63/M	R adrenal	Op	200
11	67/M	Bladder	None	200

M male, *F* female, *Op* operation, *chemo* chemotherapy, *RT* radiation therapy

FDG PET or PET/CT revealed 124 metastatic lesions in all patients (Table 2). Bone metastasis was observed in 8 of 11 patients (73%), followed by lung metastasis (64%). Liver, lymph node and retroperitoneal metastases were also observed (36%).

Table 3 summarises the data regarding ASUV, ASUV5, MSUV, summed CT diameter, serum CA, and each corresponding ratio between R and NR patients, the number of which was determined post-therapy (five and six patients, respectively). ASUV, ASUV5 and MSUV measurements were obtained for all patients, whereas the summed CT diameter and the serum CA were obtained for eight patients only. We also calculated the ratio of each index before and after therapy (Table 4). rASUV and rASUV5 were significantly different between R [rASUV 0.64 (0.18), rASUV5 0.68 (0.17)] and NR [rASUV 1.40 (0.54), rASUV5 1.37 (0.61)] patients (p=0.02 and p=0.04 for rASUV and rASUV5, respectively). Similarly, rCA was significantly different between R and NR patients (p=0.03). In contrast, rMSUV and rCT were not significantly different between R and NR patients (p=0.06 and p=0.07, respectively).

Figure 1 shows a representative case of the R patient. This patient (patient 1) underwent resection of the left adrenal mass and was treated with 100 mCi (3.7 GBq) ^{131}I-MIBG. The FDG PET/CT performed before therapy revealed intense FDG uptake of multiple metastatic lesions. Retroperitoneal metastasis and multiple lung metastases were noticed. Post-therapy FDG PET/CT revealed reduced FDG accumulation in these lesions. ASUV and ASUV5 were also decreased. Patient 7, a patient classified into the NR group, had multiple bone metastases (Fig. 2). ASUV

Table 2 Number of metastatic lesions detected by FDG PET

Patient	Metastasis				
	Bone	Lung	Liver	Retroperitoneum	Lymph node
1		++		+	
2	++	++		+	++
3	++	++	++		
4	++		++		
5	++	++			
6	++				
7		++			++
8		++		+	++
9	++		++		
10	++		++	+	
11	++	++			++

+ metastasis detected by FDG PET, ++ multiple metastases detected by FDG PET

Table 3 The disease response evaluated by different measures of pre- and post-therapy

Patients		ASUV			ASUV5			MSUV			CT diameter (mm)			Serum CA (ng/ml)		
		Pre	Post	rASUV	Pre	Post	rASUV5	Pre	Post	rMSUV	Pre	Post	rCT	Pre	Post	rCA
R	1	8.28	4.68	0.57	8.28	4.68	0.57	13.20	8.80	0.67	52.00	52.00	52.00	–	–	–
	2	5.90	2.77	0.47	11.32	7.48	0.66	16.50	12.10	0.73	101.00	91.00	0.90	8.61	4.19	0.49
	3	8.30	6.55	0.79	8.30	6.55	0.79	12.50	10.20	0.82	26.50	26.50	1.00	1.65	1.01	0.61
	4	6.01	3.01	0.50	6.78	3.32	0.49	8.60	3.00	0.35	39.00	35.00	0.90	7.71	6.08	0.79
	5	4.53	3.94	0.87	6.78	6.12	0.90	9.24	8.45	0.91	–	–	–	13.14	5.93	0.45
NR	6	2.50	4.09	1.64	2.50	4.09	1.64	3.19	3.43	1.08	189.00	189.00	1.00	0.94	2.65	2.82
	7	9.72	10.60	1.09	12.76	13.32	1.04	19.70	16.80	0.85	90.00	90.00	1.00	7.60	10.86	1.43
	8	4.53	4.76	1.05	5.74	4.27	0.74	8.69	6.36	0.73	115.00	134.00	1.17	0.70	0.65	0.93
	9	2.23	2.72	1.22	2.23	2.72	1.22	2.45	2.88	1.18	–	–	–	–	–	–
	10	3.54	8.54	2.41	3.75	9.26	2.47	4.56	8.47	1.86	–	–	–	–	–	–
	11	6.80	6.91	1.02	12.18	13.86	1.14	13.10	13.60	1.04	100.00	106.00	1.06	3.59	9.73	2.71

R responder, *NR* non-responder, *CA* norepinephrine was adopted for a catecholamine index, *CT diameter* sum of the longest diameter of five highest SUV_{max} lesions

Table 4 The ratio of pre- and post-therapy values according to the response to therapy

R responder, *NR* non-responder, *CA* norepinephrine was adopted for a catecholamine index

	rASUV	rASUV5	rMSUV	rCT	rCA
R	0.64±0.18	0.68±0.17	0.70±0.22	0.95±0.06	0.58±0.15
NR	1.40±0.54	1.37±0.61	1.12±0.34	1.06±0.08	1.97±0.94
p value	0.02	0.04	0.06	0.07	0.03

increased from 9.72 to 10.60; ASUV5 increased from 12.76 to 13.32. Serum norepinephrine levels also increased from 7.60 to 10.86 ng/ml. However, neither patient 1 nor patient 7 exhibited major changes in the size of the tumour lesions.

Discussion

^{131}I-MIBG therapy is not expected to result in remarkable tumour shrinkage or eradication in most of the patients. In malignant phaeochromocytoma, the 5-year survival rate is low. Thus, the goal of treatment is to delay disease progression and extend survival with quality of life. For the evaluation of therapeutic response, the combination of clinical, biochemical and radiological findings are estimated; however, no single parameter by which the therapeutic response is evaluable has been established. According to our study on ^{131}I-MIBG therapy evaluation, no significant difference was observed between R and NR patient groups with regard to changes in tumour size measured by CT. This is consistent with the fact that many cases do not show changes in tumour size before and after therapy. On the other hand, FDG uptake measured by SUV was significantly decreased in the R group as compared with the NR group.

At present, therapy evaluation by the Response Evaluation Criteria in Solid Tumors (RECIST) was mainly based on the measurement of length by CT. On the other hand, evaluation by the PET Response Criteria in Solid Tumors (PERCIST) has been used in recent years [15]. In the case of malignant phaeochromocytoma, anti-tumour effects are usually moderate compared with chemotherapy on common solid tumours, and tumour shrinkage is rare even in cases with improved symptoms. Therefore, it is unlikely that a significant difference was observed by CT imaging between the two groups in this study. A significant difference was observed only in the SUV, as assessed by FDG PET. Notably, evaluation is considered to be barely possible in the case of a subtle quantitative change in glucose metabolism.

The ratio of the highest SUV_{max} (rMSUV) was not significantly different between R and NR patient groups.

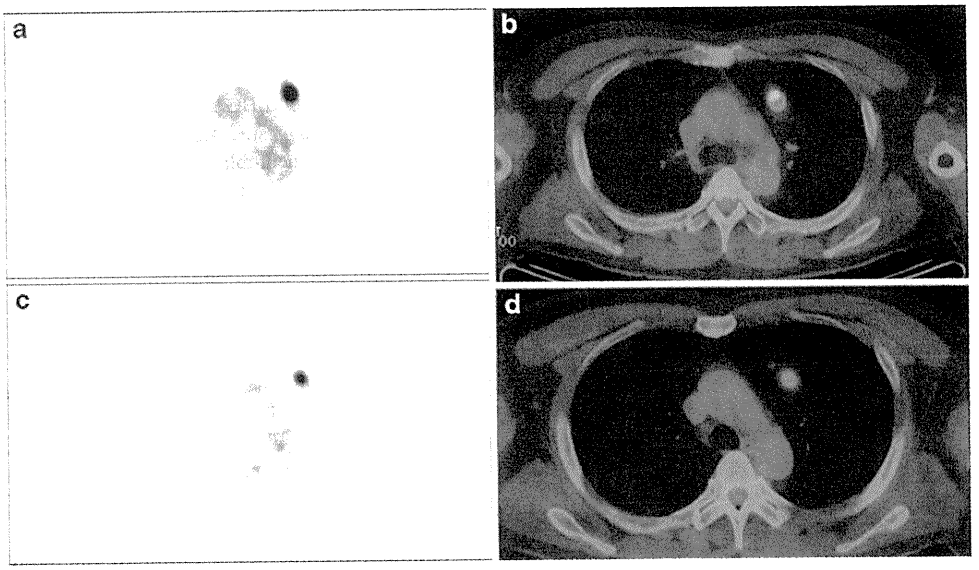

Fig. 1 A 43-year-old male patient with multiple lung metastases (patient 1). PET (**a**) and combined PET/CT (**b**) images obtained before ^{131}I-MIBG therapy showed FDG uptake in the lung metastasis. PET (**c**) and PET/CT (**d**) 3 months after ^{131}I-MIBG therapy showed FDG uptake decreased from 10.7 to 4.6

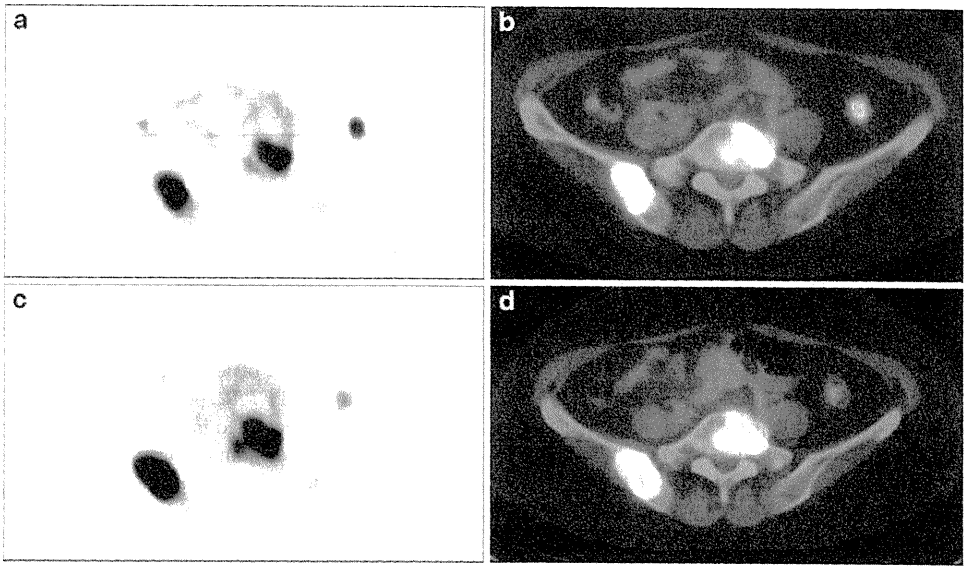

Fig. 2 A 57-year-old man (patient 7) underwent ^{131}I-MIBG therapy (200 mCi). PET (**a**) and PET/CT (**b**) images before ^{131}I-MIBG therapy showed FDG uptake in the right iliac bone and the L5 vertebra. Increased FDG uptake was also observed in the post-therapy study (from 12.8 to 17.3) (**c**, **d**)

On the other hand, a significant difference was observed for rASUV (calculated as the average of SUV changes for all lesions), or simplified rASUV5. On the basis of the above, we consider accurate evaluation to be impossible even using SUV without a comprehensive review of the accumulated changes in multiple lesions.

In our study, the most significantly different parameter between R and NR patients was rASUV. Unfortunately, in cases with a large number of metastases, determination of the SUV_{max} for all of the lesions by FDG PET is highly time-consuming. Therefore, ASUV5 (also statistically significant between R and NR patients) may be a suitable parameter for evaluation of the therapeutic effects. This method is less time-consuming than measurement of the SUV_{max} for all of the lesions.

In a study by Nwosu et al. [14], Kaplan-Meier analysis showed significantly increased survival (p=0.01) from the date of first ^{131}I-MIBG administration in patients with metastatic neuroendocrine tumours who reported symptomatic improvement. Patients with biochemical and radiological (MIBG scan, CT and MRI) responses did not show any statistically significant alteration in survival compared with NR patients. Ideally, assessment of the therapeutic effectiveness of ^{131}I-MIBG therapy should be based on Kaplan-Meier survival curves. However, these analyses are not available in malignant phaeochromocytoma because it is a rare disease, with only a few cases per year treated with ^{131}I-MIBG. In addition, evaluation of symptoms is a subjective parameter. Although the evaluation of symptoms is clinically useful, the assessment should be objective and reproducible. In our study, we used an objective method (based on SUV determination) for the quantitative evaluation of therapy response.

Our study suggests that FDG PET is useful for monitoring the efficiency of ^{131}I-MIBG therapy. However, we did not analyse MIBG scan as an evaluation procedure. Taggart et al. suggested that, for patients with MIBG-positive relapsed neuroblastoma, MIBG is more sensitive than FDG PET for disease detection and response evaluation after ^{131}I-MIBG therapy [16]. In that study, the therapeutic effect was assessed by comparing the number of lesions detected before and after ^{131}I-MIBG therapy by FDG PET coupled with MIBG scan. In malignant phaeochromocytoma, metastatic lesions rarely disappear after ^{131}I-MIBG therapy. The purpose of ^{131}I-MIBG therapy is usually to control disease progression. Therefore, it is inappropriate to use the change in the number of metastatic lesions detected by FDG PET as an evaluation method for malignant phaeochromocytoma. Therefore, our study is important because it provides a quantitative method for such evaluation.

Our study has some limitations. Firstly, the number of patients is limited. Secondly, the final assessment of therapeutic effectiveness is inadequate. Accurate definition of R and NR was important in this study. Ideally, patients should be classified into R and NR after a long-term

(several years) follow-up; however, we classified the patients after 1-year follow-up.

In conclusion, the results of the present study indicate that FDG PET is an alternative and useful method for evaluating the effect of ^{131}I-MIBG therapy as compared to CT in patients with malignant phaeochromocytoma. The change in SUV from pre- to post-therapy, as assessed by FDG PET, can be used as a quantitative index of assessment. In particular, the average SUV_{max} of the five highest lesions may be useful in the present clinical evaluation. Thus, FDG PET has the potential to predict or monitor the response to ^{131}I-MIBG therapy.

Conflicts of interest None.

References

1. Ilias I, Pacak K. A clinical overview of pheochromocytomas/paragangliomas and carcinoid tumors. Nucl Med Biol 2008;35:S27–34.
2. Lenders JW. Biochemical diagnosis of pheochromocytoma and paraganglioma. Ann Endocrinol (Paris) 2009;70:161–5.
3. Guller U, Turek J, Eubanks S, Delong ER, Oertli D, Feldman JM. Detecting pheochromocytoma: defining the most sensitive test. Ann Surg 2006;243:102–7.
4. Salmenkivi K, Heikkilä P, Haglund C, Arola J. Malignancy in pheochromocytomas. APMIS 2004;112:551–9.
5. Havekes B, Lai EW, Corssmit EP, Romijn JA, Timmers HJ, Pacak K. Detection and treatment of pheochromocytomas and paragangliomas: current standing of MIBG scintigraphy and future role of PET imaging. Q J Nucl Med Mol Imaging 2008;52:419–29.
6. John H, Ziegler WH, Hauri D, Jaeger P. Pheochromocytomas: can malignant potential be predicted? Urology 1999;53:679–83.
7. Eisenhofer G, Bornstein SR, Brouwers FM, Cheung NK, Dahia PL, de Krijger RR, et al. Malignant pheochromocytoma: current status and initiatives for future progress. Endocr Relat Cancer 2004;11:423–36.
8. Hoefnagel CA, Schornagel J, Valdés Olmos RA. [131I]metaiodobenzylguanidine therapy of malignant pheochromocytoma: interference of medication. J Nucl Biol Med 1991;35:308–12.
9. Sisson J, Shapiro B, Beierwaltes WH, Nakajo M, Glowniak J, Mangner T, et al. Treatment of malignant pheochromocytoma with a new radiopharmaceutical. Trans Assoc Am Physicians 1983;96:209–17.
10. Ackery DM, Troncone L. Session on the role of [131I]metaiodobenzylguanidine in the treatment of malignant phaeochromocytoma. Chairmen's report. J Nucl Biol Med 1991;35:318–20.
11. Safford SD, Coleman RE, Gockerman JP, Moore J, Feldman JM, Leight Jr GS, et al. Iodine-131 metaiodobenzylguanidine is an effective treatment for malignant pheochromocytoma and paraganglioma. Surgery 2003;134:956–62.
12. Gonias S, Goldsby R, Matthay KK, Hawkins R, Price D, Huberty J, et al. Phase II study of high-dose [131I]metaiodobenzylguanidine therapy for patients with metastatic pheochromocytoma and paraganglioma. J Clin Oncol 2009;27:4162–8.
13. Menzel C, Graichen S, Berner U, Risse JH, Diehl M, Döbert N, et al. Monitoring the efficacy of iodine-131-MIBG therapy using fluorine-18-FDG-PET. Acta Med Austriaca 2003;30:37–40.
14. Nwosu AC, Jones L, Vora J, Poston GJ, Vinjamuri S, Pritchard DM. Assessment of the efficacy and toxicity of (131)I-metaiodobenzylguanidine therapy for metastatic neuroendocrine tumours. Br J Cancer 2008;98:1053–8.
15. Wahl RL, Jacene H, Kasamon Y, Lodge MA. From RECIST to PERCIST: evolving considerations for PET response criteria in solid tumors. J Nucl Med 2009;50:122S–50.
16. Taggart DR, Han MM, Quach A, Groshen S, Ye W, Villablanca JG, et al. Comparison of iodine-123 metaiodobenzylguanidine (MIBG) scan and [18F]fluorodeoxyglucose positron emission tomography to evaluate response after iodine-131 MIBG therapy for relapsed neuroblastoma. J Clin Oncol 2009;27:5343–9.

INTERNATIONAL JOURNAL OF
UROLOGY

International Journal of Urology (2012) doi: 10.1111/j.1442-2042.2011.02950.x

Case Report

Pheochromocytoma crisis caused by *Campylobacter fetus*

Ichiro Abe,[1] Masatoshi Nomura,[1] Makiko Watanabe,[1] Shingo Shimada,[2] Michiko Kohno,[1] Yayoi Matsuda,[1] Masahiro Adachi,[1] Hisaya Kawate,[1] Keizo Ohnaka[1] and Ryoichi Takayanagi[1]

[1]Department of Medicine and Bioregulatory Science, Graduate School of Medical Science, Kyushu University, Fukuoka, and [2]Department of Internal Medicine, Kyushu Rosai Hospital, Labor Welfare Corporation, Kitakyushu, Japan

Abbreviations & Acronyms
CRP = C-reactive protein
DBP = diastolic blood pressure
SBP = systolic blood pressure

Correspondence: Masatoshi Nomura M.D., Ph.D., Department of Medicine and Bioregulatory Science, Graduate School of Medical Science, Kyushu University, Maidashi 3-1-1, Higashi-ku, Fukuoka 812-8582, Japan. Email: nomura@med.kyushu-u.ac.jp

Received 30 August 2011; accepted 11 December 2011.

Abstract: Pheochromocytoma crisis is a life-threatening endocrine emergency associated with symptoms of excess release of catecholamines. It might present spontaneously or be unmasked by triggers including trauma, surgery and certain medications that provoke catecholamine release by tumors. Here we report a case of pheochromocytoma crisis associated with abscess formation in the tumor and bacteremia of *Campylobacter fetus*, which was successfully treated with antibiotics and a surgical resection. This case appears to be the first reported case in the literature of abscess formation by *C. fetus* in pheochromocytoma, leading to catecholamine crisis.

Key words: abscess, antibiotics, *Campylobacter fetus*, catecholamine crisis, pheochromocytoma.

Introduction

Pheochromocytoma crisis is a rare, life-threatening endocrine emergency associated with symptoms of excess release of catecholamines by the tumor. It might present spontaneously or be unmasked by triggers, such as trauma, surgery, anesthesia, drug therapy and infection. Catecholamine crisis has several manifestation components including multiple organ failure, severe blood pressure variability, encephalopathy and high fever. A constellation of very dramatic manifestations occurs, which are progressive despite intensive medical management and lead to multiorgan failure. Consequently, a delay in making a definitive diagnosis and carrying out appropriate therapy results in further deterioration of the patient's condition. Therefore, it is important to recognize pheochromocytoma crisis as an emergency condition and to carry out thorough searches for coexisting diseases for proper diagnosis and treatment. It is uncommon for fever to be the presenting manifestation of pheochromocytoma. However, high fever is a common manifestation of pheochromocytoma crisis. The causes of fever might be multifactorial and often include an associated illness, most likely an infectious disease.

Campylobacter fetus is rarely isolated from humans, although it is ubiquitous in cattle, pigs and poultry. It is usually associated with opportunistic infections. Here, we report a case of pheochromocytoma crisis associated with abscess formation in the tumor and bacteremia of *C. fetus*, which was successfully treated with antibiotics and a surgical resection.

Case report

A 53-year-old woman was admitted with complaints of high fever, fatigue and stagger for 1 week. She had experienced a subarachnoid hemorrhage 2 years previously. Thereafter, she had been treated for hypertension. She was diagnosed with type 2 diabetes 6 months earlier. On physical examination, she presented with variable systolic blood pressure ranging from 120 to 220 mmHg. Her body temperature was 38.0°C, and her pulse rate was 110/min and regular. Her skin appeared normal, except for extreme perspiration. Laboratory tests showed

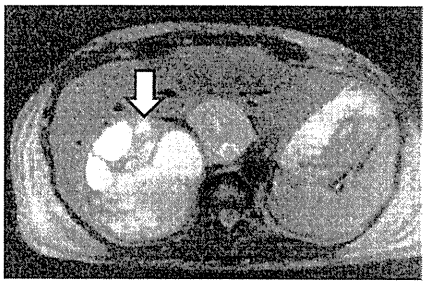

Fig. 1 Magnetic resonance imaging showed a huge mass with high density and a relatively low-density area on T2W1 (arrow).

an elevated white blood cell count of 13 230/mm^3, with 86.5% neutrophils and C-reactive protein of 19.91 mg/dL. The hemoglobin level was 9.5 g/dL and the platelet count was 335 000/mm^3. On biochemical investigation, blood glucose was 184 mg/dL and glycated hemoglobin was 6.8%. Abdominal computed tomography showed a huge right adrenal mass (12 × 14 cm in diameter) with a low-density area. Magnetic resonance imaging showed a high-density area on T2W1, suggesting bleeding and/or necrosis (Fig. 1). As pheochromocytoma was highly suspected, an endocrinological investigation was carried out. As expected, highly elevated plasma catecholamines as well as urine catecholamines and metanephrine became evident. The patient's plasma adrenaline was 21 984 pg/mL, plasma noradrenaline 53 696 pg/mL, plasma dopamine 766 pg/mL, urine adrenaline 186 μg/day, urine noradrenaline 333.3 μg/day, urine dopamine 759.8 μg/day, urine metanephrine 5.37 mg/day and urine normetanephrine 1.95 mg/day. The abnormal uptake in a ^{131}I-meta-iodobenzylguanidine scan was compatible with pheochromocytoma of the right adrenal gland (data not shown). To exclude the possibility of an associated infectious disease as a cause of fever, a blood culture test was carried out. Surprisingly, *C. fetus* was detected in the blood culture. Based on these findings, a diagnosis of pheochromocytoma crisis and bacteremia of *C. fetus* was made. Therefore, we commenced treatment with antibiotics (initially meropenem and then ciprofloxacin), together with a high dose of alpha-blocker followed by a low dose of beta-blocker. As a result of the treatment, her condition improved sufficiently to allow an operation, and she underwent an open surgery for right adrenalectomy (Fig. 2a). The operative time was 3 h 23 min and estimated blood loss was 1030 g, leading to intraoperative blood transfusion with 6 U of red cell concentrates. Monitoring the change in blood pressure showed a transient increase of systolic blood pressure by 50 mmHg during operation. After the operation, her clinical signs of sustained blood pressure variability were dramatically improved and the alpha-blocker was discontinued, as summarized in Figure 3. In addition, her glucose metabolism was normalized. Histological examination of the excised specimen showed a proliferation of polygonal cells with round or irregular nuclei, and a granular cytoplasm arranged in sheets and a trabecular fashion, accompanied by an irregular fibrous septum and hemorrhagic change. Immunohistochemistry showed that the tumor cells were positive for chromogranin A, synaptophysin, CD56, S-100 and NSE. The MIB-1 index was approximately 3%. An abscess with neutrophil infiltration was seen at the center of the tumor (Fig. 2b), and necrosis was concomitant. To determine the etiology of the abscess, fluid samples from the abscess and a crushed specimen were cultured, and *C. fetus* was identified. Collectively, pheochromocytoma crisis caused by abscess formation in the tumor and bacteremia of *C. fetus* was diagnosed.

Discussion

Pheochromocytoma crisis is a rare life-threatening endocrine emergency with a reported mortality as high as 85%. Acute and rapidly progressive hemodynamic disturbances result from the actions of high quantities of catecholamines leading to multiple organ failure.[1,2] Pheochromocytoma crisis can be caused by triggers such as trauma, surgery, anesthesia, drug therapy and infection.[3]

Generally, abscess formation can occur in a variety of organs in compromised hosts. It has been reported that abscess formation in the adrenal gland can be induced by placental infection and lead to adrenal hemorrhage.[4,5] However, abscesses in pheochromocytoma are quite rare and, to the best of our knowledge, there are just three previously reported cases.[6–8] Two of these cases presented with fever and variable blood pressure compatible with pheochromocytoma crisis. The other case presented with high fever, but normal blood pressure. Regarding the etiology, the abscess formations were caused by *Salmonella typhimurium* in two cases and *Streptococcus agalactiae* in the other case. In the present case, the abscess formation was caused by *C. fetus*, which is usually associated with opportunistic infections.[9] As *C. fetus* infection usually occurs in patients with immunosuppressive conditions, it leads to a prolonged clinical course and higher mortality. The mechanism of *C. fetus* infection is barely understood, except that it penetrates from the intestinal tract. Some cases of *C. fetus* infection have been reported to be caused by eating fresh liver from cattle or pigs.[10] Indeed, in the present case, the patient ate fresh bovine liver before showing the symptoms. Pheochromocytoma crisis might be considered to be an immunosuppressive disorder.

With regard to abscess formation by *C. fetus*, there are reports of abscesses in various organs including the brain, lung and colon, but not in the adrenal gland. We have reported the first case of pheochromocytoma with an

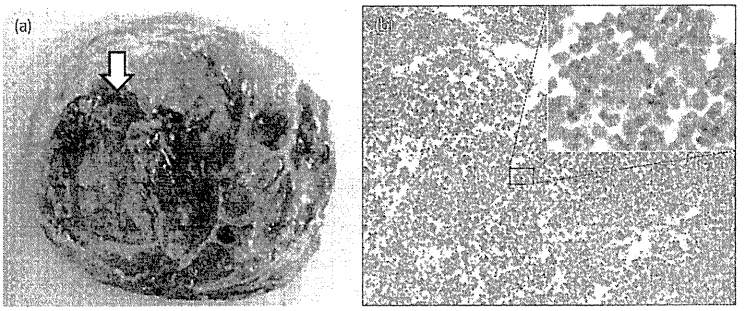

Fig. 2 Abscess formation in the tumor. (a) The excised specimen shows both solid parts and hollow parts suggesting the presence of an abscess (arrow). (b) Hematoxylin–eosin staining of the specimen shows an abscess with neutrophilic infiltration. (Inset) A high magnification image taken from the area indicated by rectangle.

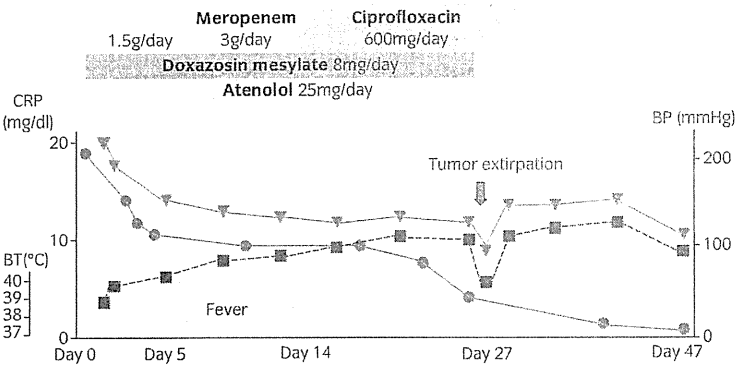

Fig. 3 Clinical course of the patient. On admission to our hospital, the patient presented with fever and variable systolic pressure ranging from 120 to 220 mmHg. Her C-reactive protein level was also high. She was successfully treated with antibiotics and a high dose of alpha-blocker followed by extirpation of her pheochromocytoma. —●—, CRP; —▼—, SBP; --■--, DBP; , Fever.

abscess caused by *C. fetus*. Based on the clinical course of the patient, it is likely that abscess formation in the tumor and bacteremia of *C. fetus* can cause pheochromocytoma crisis. Therefore, the present case is very suggestive in terms of the etiology of pheochromocytoma crisis. We should consider the possibility of abscess formation in the tumor and bacteremia of *C. fetus* in febrile patients with pheochromocytoma crisis for the best treatment with antibiotics.

Conflict of interest

None declared.

References

1 Browers FM, Lenders JW, Eisenhofer G, Pacak K. Pheochromocytoma as an endocrine emergency. *Rev. Endocr. Metab. Disord.* 2003; **4**: 121–8.

2 Sauvage MR, Tulasne PA, Arnaud JP. Hypertensive accident in a surgical patient with unsuspected pheochromocytoma. *Anesth. Analg.* 1979; **36**: 155–8.

3 Newell K, Prinz RA, Braithwaite S, Brooks M. Pheochromocytoma crisis. *Am. J. Hypertens.* 1988; **1**: 189–91.

4 Suri S, Agarwalla ML, Mitra SK, Bhagwat AG. Adrenal abscess in a neonate presenting as a renal neoplasm. *Br. J. Urol.* 1982; **54**: 565.

5 Steffens J, Zaubitzer T, Kirsch W, Humke U. Neonatal adrenal abscesses. *Eur. Urol.* 1997; **31**: 347–9.

6 Giel CP. An abscess formation in a pheochromocytoma; report of a case due to Salmonella typhimurium. *N. Engl. J. Med.* 1954; **251**: 980–2.

7 Ulm AH, Rudansky S, Senger FL. Metastatic abscess of pheochromocytoma. *J. Urol.* 1955; **73**: 901–5.

8 Inoue R, Hisasue S, Kunishima Y, Masumori N, Itoh N, Tsukamoto T. Pheochromocytoma with abscess. *Int. J. Urol.* 2007; **14**: 644–6.

9 Zonis DI, Panayiotakopoulos GD, Kabletsas EO, Tzima EL, Stefanou I, Archimandritis AJ. Campylobacter Fetus bacteraemia in a healthy individual: clinical and therapeutical implications. *J. Infect.* 2005; **51**: 329–32.

10 Ichiyama S, Hirai S *et al.* Campylobacter Fetus subspecies Fetus cellulitis associated with bacteremia in debilitated hosts. *Clin. Infect. Dis.* 1998; **27**: 252–5.

3　MIBG シンチグラフィ

金沢大学医薬保健研究域医学系核医学　絹谷清剛

臨床医のための Point

❶褐色細胞腫イメージ用には ^{131}I-MIBG と ^{123}I-MIBG の２種類がある．
❷画質がよく，被曝線量が少ないため ^{123}I-MIBG シンチグラフィが望ましい．
❸ ^{123}I-MIBG では SPECT 撮像が可能である．正確な病巣部位把握には SPECT 撮像が有用である．
❹ SPECT/CT fusion 画像が有用である．

◎検査の目的

①副腎腫瘤が存在する症例における鑑別診断．
②症状・検査所見から褐色細胞腫・傍神経節腫の存在が疑われる場合の存在診断．
③褐色細胞腫の確定診断が得られた症例における転移存在診断．
④治療効果判定・経過観察．

◎前処置

①^{131}I-meta-iodobenzylguranidine（MIBG）では，無機ヨード投与による甲状腺ブロックを実施する．^{123}I-MIBG では，被曝の点からは甲状腺ブロックの必要性は低いものの，随伴する可能性のある甲状腺髄様癌の誤認を避けるためにブロックすることが望ましい．甲状腺ブロックの定まった手法はないが，MIBG 投与１～３日前から３日間程度，ヨウ化カリウム丸１錠，ルゴール液１mL を内服させるのが一般的である．
②向精神薬などが MIBG の病巣集積を阻害しうるため，当該薬剤は MIBG シンチグラフィ１～２週前に休薬とする[1]．

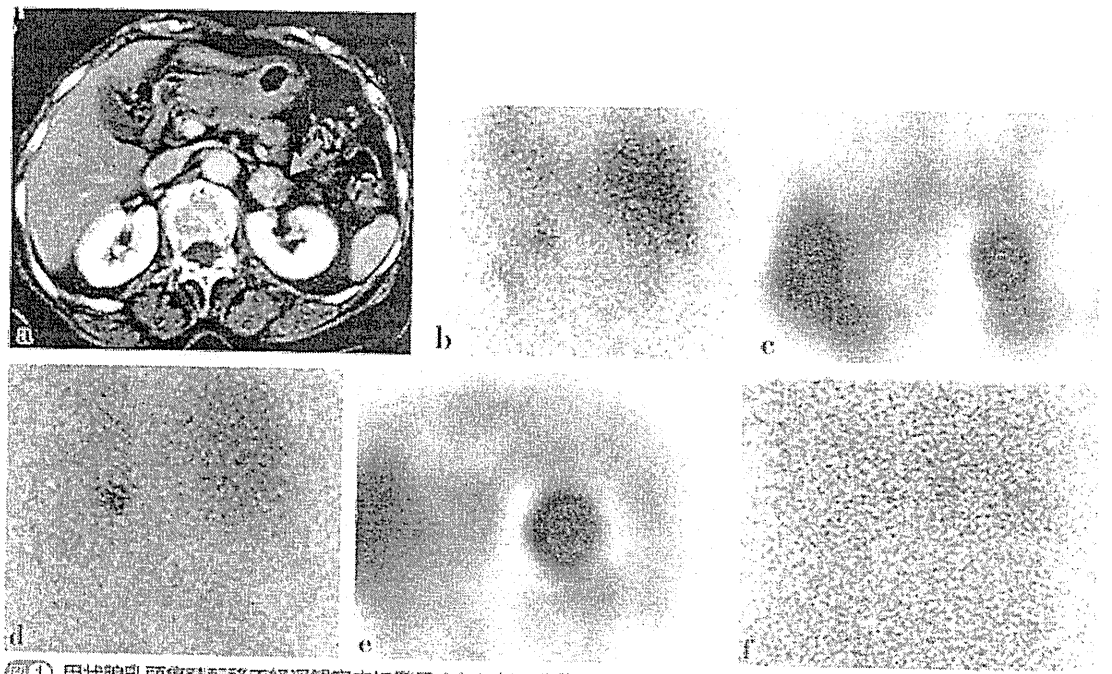

図① 甲状腺乳頭癌肺転移で経過観察中に発見された褐色細胞腫
造影 X 線 CT で，左副腎に造影効果を示す腫瘤を認める(a)．^{123}I-MIBG の投与６時間後の腹部後面像(b)・SPECT 像(c)，24 時間後の腹部背面像(d)・SPECT 像(e)で，当該腫瘤に MIBG 集積が明らかである．24 時間像のほうが描画が良好である．副腎皮質描画製剤の ^{131}I-アドステロール（投与６日後後面像）では腫瘤への集積は認められない（正常右副腎が淡く描画されている）(f)．副腎皮質機能，髄質機能ともに異常は認められなかった症例であり，シンチグラム所見が鑑別診断に有用であった．

実施方法

①^{131}I-MIBG では静注 2～3 日後に撮像する．以前はスポット撮影が主であったが，最近は全身像の撮影をすることが多い．
②^{123}I-MIBG では静注 6 時間後と 24 時間後に全身像を撮像する．SPECT 撮像を適宜追加する．

所見・診断

①病巣部位への集積を認めれば，褐色細胞腫に代表される神経内分泌腫瘍と診断可能である(図 1)．
②^{123}I-MIBG のほうが，投与量が多いことやガンマカメラでの撮像に適したγ線エネルギーであることなどから，^{131}I-MIBG よりも画質がすぐれている傾向にある(図 2)．
③一般的に，遅い時間での撮像のほうがコントラストが良好である(図 1，3)．
④^{131}I-MIBG 内用療法施行時のシンチグラムで，検査時シンチグラムで検出されない病巣が検出されることが多くの症例で経験される．治療時の MIBG 投与量が多いことと，治療時シンチグラフィ撮像が投与後 4 日目以降になることが多く，バックグラウンドとのコントラストが良好になるために起こる現象である(図 4)．
⑤SPECT 画像の追加により，部位同定が容易になる．特に CT との fusion 画像を作成することにより，診断能の向上が見込める(図 3，4)．
⑥甲状腺ブロックを行っても，十分にブロックしきれない症例もある(図 5)．

検査に伴う対応

授乳中の女性では，検査後しかるべき期間，授乳を控えるよう指導する．^{123}I-MIBG では 2 日間，^{131}I-MIBG では 3 週間である．

補　足

褐色細胞腫に保険適用があるのは従来は ^{131}I-MIBG だけであったが，最近 ^{123}I-MIBG が褐色細胞腫にも保険適用が拡大されるよう検討された．^{123}I-MIBG では 222 MBq までの投与が可能である．検出能向上のためには 222 MBq 投与が望ましい．

● 文 献
1) 日本核医学会分科会腫瘍・免疫核医学研究会：^{131}I-MIBG 内照射療法ガイドライン作成委員会：神経内分泌腫瘍に対する ^{131}I-MIBG 内照射療法の適正使用ガイドライン集．核医学 2008；45：別 1-40．

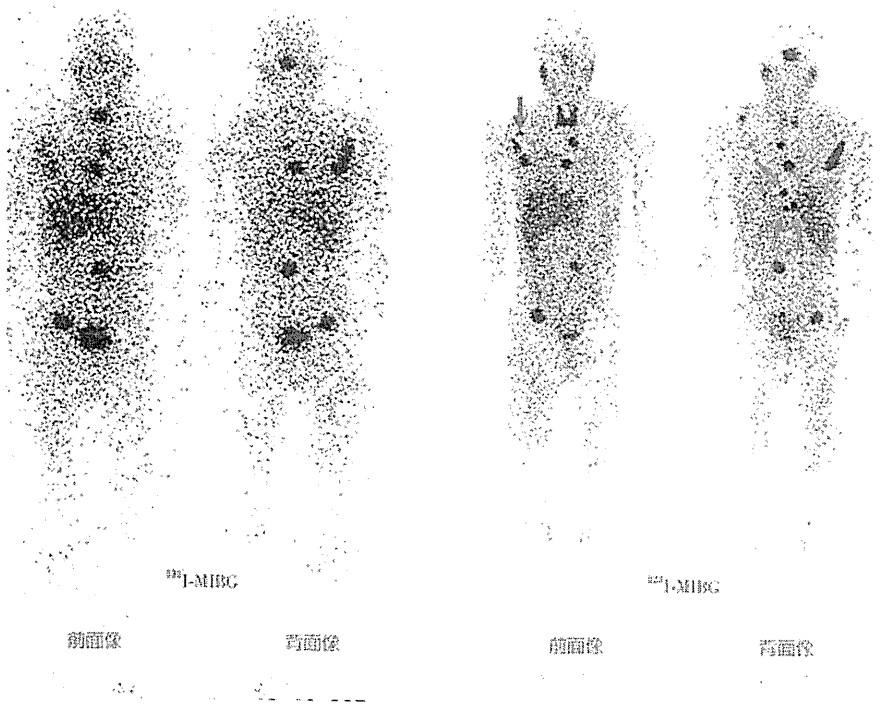

図② 診断投与量 ^{131}I-MIBG シンチグラムと ^{123}I-MIBG シンチグラムの比較
^{123}I-MIBG シンチグラムのほうが解像度にすぐれる．^{131}I-MIBG でのみ認識される病巣(矢印)があることに注目．